Experimental observation of the nonequivalence of rotation of the magnetic moments of the sublattices in antiferromagnetic $FeCl_2$ in a transverse magnetic field

A. N. Bazhan and V. A. Ul'yanov[1]

Institute of Physical Problems, Academy of Sciences, USSR

(Submitted 7 December 1979)
Zh. Eksp. Teor. Fiz. **79**, 186–193 (July 1980)

The phase transition in the easy-axis antiferromagnet $FeCl_2$ has been investigated in magnetic fields H up to 65 kOe, at temperature $T = 4.2$ K, in the case in which the magnetic field H is perpendicular to the trigonal axis. The vibrating-sample magnetometer used permitted measurement of mutually perpendicular components of the magnetic moment of the specimen. A magnetic moment of the specimen along the trigonal axis C_3 was detected; it had a 120-degree periodicity on variation of the orientation of the applied magnetic field in the basal plane of the crystal, perpendicular to this axis.

PACS numbers: 75.30.Kz, 75.50.Ee

The rhombohedral easy-axis antiferromagnet $FeCl_2$, of symmetry D_{3d}^5, with two ions in the elementary cell (Fig. 1), is among the quite thoroughly studied materials.[1-7] It is a metamagnetic material; because of the different values of the exchange interaction within the sublattices and between the sublattices, there occurs in it a metamagnetic phase transition from the antiferromagnetic to a ferromagnetic state at field $H = 12$ kOe, when the magnetic field H is directed along the trigonal axis C_3 (along the antiferromagnetic vector).[1] When the magnetic field is oriented perpendicular to the trigonal axis, a phase transition from the antiferromagnetic to the ferromagnetic state occurs at magnetic field $H = 120$ kOe.[2]

The phase transitions in $FeCl_2$ have been studied in considerable detail by various methods. Papers have been published recently on investigation of the Mössbauer effect[4] and on measurement of the polarization of a neutron beam after passage through an $FeCl_2$ specimen.[5] These experiments[4,5] can be explained by the presence of a component of the magnetic moment of the specimen along the trigonal axis C_3 when the applied magnetic field is oriented in a direction perpendicular to this axis. In this connection, it is of interest to carry out a direct experimental observation and investigation of the magnetic moment along the trigonal axis C_3 of an $FeCl_2$ specimen[2] in a transverse magnetic field, on a magnetometer that permits measurement of the magnetic moment of the specimen along three mutually perpendicular directions.[6]

EXPERIMENTAL RESULTS

In order to describe the experiments carried out on the magnetometer, we choose a system of coordinates for the orientations of the magnetic field, of the crystal axes, and of the axes of magnetic-moment measurement in the apparatus. Let axes x, y, z be attached to the directions of measurement of the magnetic moment in the apparatus; then we denote by $M_i(H_j)$ the magnetic moment measured along the direction $j(x, y, z)$ when the applied magnetic field is oriented along the direction $j(x, y, z)$. We fix the crystallographic directions of the specimen in the x, y, z system as follows: $z \| C_3, x \| C_2$, where C_3 is the trigonal and C_2 a binary axis of the single crystal. This notation simplifies the description of the experiments on measurement of the components of the magnetic moment of the crystal for various orientations of the applied magnetic field with respect to the crystal axes.

Figure 2 (Curve 1) shows the variation of the magnetic moment $M_z(H_z)$ of the specimen along the applied magnetic field when the latter is oriented along the trigonal axis. In agreement with the papers of other authors,[1-3] there occurs at field $H = H_e = 12$ kOe a metamagnetic phase transition from the antiferromagnetic to a ferromagnetic state. At magnetic field $H < 10$ kOe, the $M_z(H_z)$ relation is described by the expression $M(H) = \chi^* H$, where $\chi^* = (1.1 \pm 0.1) \cdot 10^{-2}$ cgs emu/mol; at $H > 17$ kOe, the $M_z(H_z)$ relation is described by the expression $M(H) = 2M_0$, where M_0 is the saturation magnetic moment of the Fe^{++} ion of a single sublattice. Curve 2 in Fig. 2 represents the variation of the magnetic moment $M_z(H_z)$ of the specimen measured in the basal plane of the crystal during this phase transition. It is evident from Fig. 2 that in the phase-transition

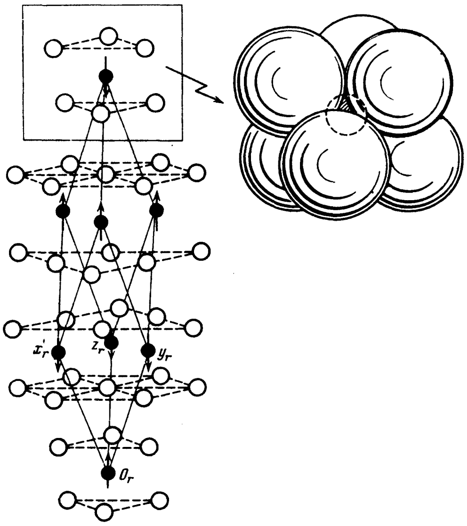

FIG. 1. Elementary cell of $FeCl_2$: ○, Cl^- ions; ●, Fe^{++} ions.

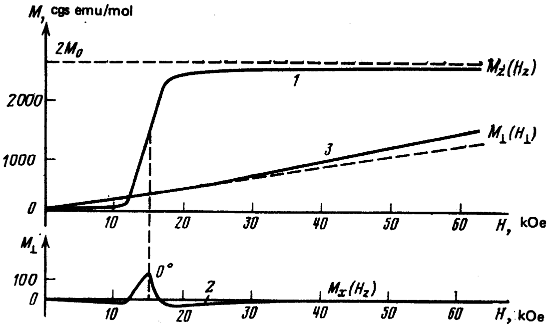

FIG. 2. Field dependence of the magnetic moment $M_z(H_z)$ measured along the applied magnetic field H for orientations H $\| C_3$, Curve 1, and H$\perp C_3$, Curve 3; and of the magnetic moment $M_x(H_z)$ measured perpendicular to the applied magnetic field for orientation H$\| C_3$, Curve 2. The dotted straight line corresponds to the doubled saturation moment of the Fe^{++} ions.

region, there is observed on the $M_x(H_z)$ curve the appearance of a magnetic moment quite strongly dependent on the orientation of the magnetic field H with respect to the trigonal axis. In the antiferromagnetic phase $H < 10$ kOe and in the ferromagnetic phase $H > 17$ kOe, the magnetic moment $M_x(H_z)$ in the basal plane is zero. All the further experiments were done with orientation of the magnetic field H in the basal plane of the crystal.

In Fig. 2, curve 3 represents the variation of the magnetic moment $M_\perp(H_\perp)$ of the specimen measured along the applied magnetic field H for various orientations of H in the basal plane, perpendicular to the axis C_3. It is evident from the figure that within the magnetic-field interval investigated, the relation has a weakly expressed nonlinear character on increase of the magnetic field. At magnetic field $H = 65$ kOe, the departure from the linear relation $M_\perp(H_\perp) = \chi H$, where $\chi = (1.7 \pm 0.1) \cdot 10^{-1}$ cgs emu/mol, has a value of the order of 10%. It should be noted that, as is evident from Fig. 2, on change of the orientation of the magnetic field H in the basal plane of the crystal the field dependence $M_\perp(H_\perp)$ of the magnetic moment remains practically unchanged.

Figure 3a represents the variation $M_z(H_\perp)$ of the magnetic moment measured along the trigonal axis C_3, for various orientations of a magnetic field H applied in the basal plane of the crystal. It is evident from the figure that upon application of a magnetic field H in the basal plane of the crystal, there appears a magnetic moment along its trigonal axis C_3. The magnitude and sign of this moment depend substantially on the orientation of H in the basal plane. The $M_z(H_\perp)$ relation in this case is significantly nonlinear.

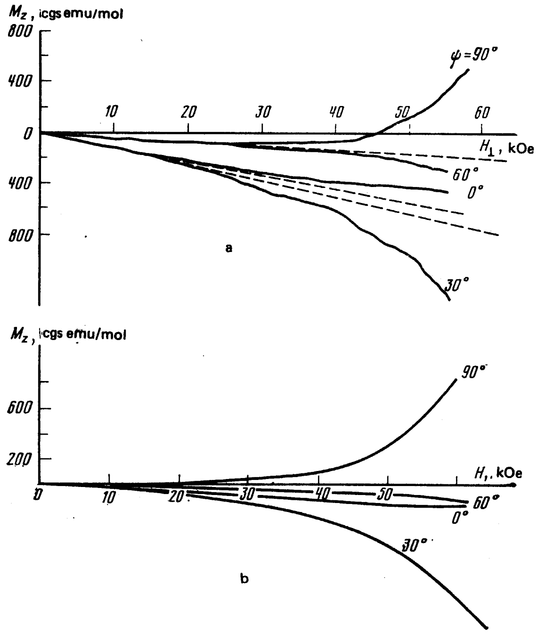

FIG. 3. a, Field dependence $M_z(H_\perp)$ of the magnetic moment measured along the vertical axis z (the trigonal axis C_3) for various orientations of an applied magnetic field H in the plane perpendicular to the axis C_3; ψ is the angle between the direction of H and the binary axis C_2. b, Field dependence $M_z(H_\perp)$ of the magnetic moment measured along the trigonal axis C_3, with allowance for inaccuracy of orientation of the vertical measurement axis z and of the trigonal axis C_3, for various or orientations of H in the plane perpendicular to the axis C_3.

For a magnetic field H oriented along a binary axis C_2, the field-dependence $M_z(H_x)$ is described by the expression $M_z(H_x) = \chi_I H + \chi_{II} H^\alpha$. For a magnetic field oriented at angle 30° to a binary axis C_2, along a vertical symmetry plane, the $M_z(H_y)$ relation is described by the relation $M_z(H_y) = \chi^{**} H$.

As a supplement to the experiment represented in Fig. 3a, Fig. 4 (Curve 1) represents the dependence of the magnetic moment of the specimen measured along the axis C_3 on the value of the angle ψ between the direction of a magnetic field applied in the basal plane and the

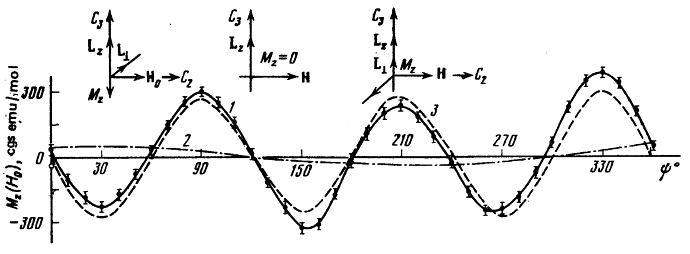

FIG. 4. Dependence of the magnetic moment $M_z(\psi)$ measured along the axis C_3, at $H_0 = 50$ kOe, on the orientation of the magnetic field in the basal plane of the crystal: Curve 1, without allowance for misorientation of the vertical measurement axis z and of the trigonal axis C_3; Curve 3, with allowance for misorientation. Curve 2 represents the allowance for the misorientation of the vertical axis z and of the trigonal axis C_3.

binary axis C_2 of the crystal. Here the value of the applied constant magnetic field is $H_0 = 50$ kOe. From this figure it is also evident that the magntidue and sign of the magnetic moment $M_z(\psi)$ vary substantially with the orientation of H in the basal plane of the crystal. In Fig. 4, the periodicity of the magnetic moment $M_z(\psi)$ as dependent on the orientation of $H_\perp$ clearly manifests itself.

A. Discussion of results

Investigation of the metamagnetic phase transition in $FeCl_2$, as has already been indicated, has been carried out in considerable detail.[1-4] In dicussion of the experiment represented in Fig. 2, one can say only that the strong dependence of the magnetic moment $M_z(H_z)$, in the region of the phase transition at $H_c = 12$ kOe, on the orientation of the magnetic field H with respect to the axis C_3, just as in previous work,[1-3] indicates that the phase transition occurs with splitting of the single crystal into magnetic domains.

We shall hereafter discuss the experiments on investigation of the phase transition in $FeCl_2$ in a transverse magnetic field.

For a magnetic field H oriented in the basal plane of the crystal, there occurs with increase of the field a rotation of the magnetic moments of the sublattices toward the direction of the applied field; this is completed at magnetic field $H = H_c^{\mathrm{II}} = 120$ kOe,[2] where there occurs a phase transition from the antiferromagnetic to the paramagnetic state. The appreciable value of the magnetic moment $M_\perp(H_\perp)$ for $H \parallel C_3$ is characteristic of the rotation of the magnetic moments of the sublattices; but the fact that the magnetic moment $M_\perp(H_\perp)$ of the specimen is practically independent of the orientation of the magnetic field in the basal plane (see Ref. 2 and Curve 3 of Fig. 2) makes it impossible, by use of these data alone, to determine the phenomena accompanying this phase transition. Use of our method makes it possible to observe the magnetic moment of the specimen that appears along the trigonal axis for definite orientations of the magnetic field H in the basal plane.

In order to determine the law that governs the change both of the magnitude of the sign of the magnetic moment $M_z(H_\perp)$ of the specimen along the axis C_3 (Figs. 3 and 4) with the value and orientation of the magnetic field H, applied in the basal plane, it is necessary to take into account, as was done in Ref. 8, the contribution to the magnetic moment $M_z(H_\perp)$ from the components of the magnetic moment of the specimen in the basal plane $M_\perp(H_\perp)$. Such a contribution arises because of inexact orientation of the specimen in the apparatus and inexact orthogonality of the applied magnetic field to the trigonal axis C_3. This contribution is easily taken into account by comparing the field-dependence of the magnetic moment $M_\perp(H_\perp)$ (Fig. 2) and the linear dependences of the magnetic moments $M_z(H_\perp)$ (Fig. 3a). The linear relations $M_z(H_\parallel)$ are described by the expression $M_z(H_\perp) = kM_\perp(H_\perp) = \chi_\perp H = k\chi H$, where k depends on the orientation of the magnetic field H with respect to the axis C_3. By subtracting from the value of the magnetic moment $M_z(H_\perp)$ the linear contribution of the magnetic moment $M_\perp(H_\perp)$, we have plotted the $M_z(H_\perp)$ relation (Fig. 3b) for various orientations of the magnetic field in the basal plane and the $M_z(\psi)$ relation at magnetic field $H_0 = 50$ kOe (Fig. 4, Curve 3). From Figs 3b and 4 it is evident that on change of the orientation of an applied magnetic field H in the basal plane of the crystal, the magnetic moment along the axis C_3 changes according to a periodic law with period 120°; that is, the dependence of the magnetic moment along the axis C_3 on the orientation of a constant-magnitude magnetic field H applied in the basal plane can be described by the expression $M_z(\psi) = M_z(H_0)\sin 3\psi$, where ψ is the angle between the direction of H and the binary axis C_2 of the crystal.

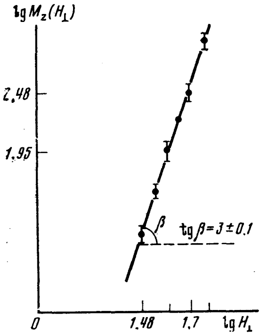

FIG. 5. Dependence of $\log M_z(H_\perp)$ on $\log H_\perp$.

In order to determine the nature of the nonlinearity $M_z(H_\perp) = \chi_{\mathrm{II}} H^\alpha$ (see Fig. 3), we plotted the variation of the value of $\log M_z(H_\perp)$ with the logarithm of the value of the applied magnetic field, $\log H_\perp$, Fig. 5. From the figure it is evident that the variation obtained is linear and that the value of the parameter $\alpha = \tan\beta$ is $\alpha = 3 \pm 0.1$. Thus the nonlinear nature of the magnetization $M_z(H_\perp)$ for orientation of H along the binary axis C_2 is determined by the law $M_z(H_x) = \chi_{\mathrm{II}} H^3$, where $\chi_{\mathrm{II}} = (2 \pm 0.4) \cdot 10^{-3}$ cgs emu/mol.

In order to determine the values of the effective fields responsible for the above-described rotation properties of the magnetic moments of the sublattices, it is necessary to do for crystals of symmetry D_{3d}^5 what was done by Dzyaloshinskiĭ[9] for crystals of symmetry D_{3d}^6: to write the thermodynamic potential describing the magnetic properties of the crystal. It must be noted that the above-indicated rotation properties can be described within the framework of the theory set forth in the papers of Nasser and Varret;[4,10] but we shall carry out an interpretation of the data on the basis of a magnetic thermodynamic potential.

The indicated magnetic properties represent a thermodynamic potential of the form

$$\begin{aligned}\Phi = {}&{}^1/_2 B\mathbf{m}^2 L_0^2 + {}^1/_2 D(\boldsymbol{\gamma}\mathbf{m})^2 L_0^4 - e(\gamma_x m_y \\ &- \gamma_y m_x) L_0^2 - {}^1/_2 i L_0^4 f[(\gamma_x + i\gamma_y)^3 - (\gamma_x - i\gamma_y)^3]\gamma_z \\ &- {}^1/_2 L_0^4 d[(\gamma_x + i\gamma_y)^3 + (\gamma_x - i\gamma_y)^3] m_z \\ &+ {}^1/_2 a\gamma_z^2 L_0^2 - \mathbf{mH}L_0,\end{aligned} \tag{1}$$

where $\mathbf{m} = (\mathbf{M}_1 + \mathbf{M}_2)/2M_0$ is the magnetic unit vector, $\gamma = (\mathbf{M}_1 - \mathbf{M}_2)/2M_0$ is the antiferromagnetic unit vector, $\mathbf{L} = \mathbf{M}_1 - \mathbf{M}_2$ is the antiferromagnetic vector, M_0 is the saturation magnetic moment of the Fe^{++} ion sublattices, and $L_0 = 2M_0$.

By minimizing the thermodynamic potential (1) with respect to m_x, m_y, and m_z, one can obtain expressions for the components of the magnetization of the specimen:

$$\begin{gathered} m_x = -\frac{D}{B+D}\frac{(\mathbf{H}\boldsymbol{\gamma})}{B}\gamma_x L_0, \\ m_y = -\frac{D}{B+D}\frac{(\mathbf{H}\boldsymbol{\gamma})}{B}\gamma_y L_0 + \frac{H}{B}, \\ m_z = -\frac{D}{B+D}\frac{(\mathbf{H}\boldsymbol{\gamma})}{B}\gamma_z L_0 + \frac{d}{B}[(\gamma_x + i\gamma_y)^3 + (\gamma_x - i\gamma_y)^3] L_0^2. \end{gathered} \tag{2}$$

Here the magnetic field is oriented in the basal plane of the crystal.

By substituting the expression (2) in (1) and then minimizing the thermodynamic potential with respect to γ_x, γ_y, and γ_z, one can obtain equations of rotation of the antiferromagnetic vector **L** with respect to crystallographic directions during increase of the applied magnetic field H for various orientations of H in the basal plane of the crystal; but unique determination of the direction of rotation of the antiferromagnetic vector **L** with respect to the crystal axes, from the experimental data presented, presents considerable difficulties.

In order to explain the origin of a nonlinear magnetic moment of the specimen along the axis C_3 for certain orientations of the applied magnetic field $\mathbf{H} \perp C_3$, we shall restrict ourselves, as was done earlier,[8] to consideration in the thermodynamic potential (1) of the invariant $\frac{1}{2}d[(\gamma_x + i\gamma_y)^3 - (\gamma_x - i\gamma_y)^3]m_z$, which is responsible for the occurrence of a magnetic moment of the specimen along the axis C_3 when there is a component of the antiferromagnetic vector **L** in the basal plane of the crystal. Then the variation of this magnetic moment with the applied magnetic field is determined by the expression

$$m_z = (d/B) L_0^2 \sin^3\theta \cos 3\varphi, \tag{3}$$

where θ is the angle between the direction of the antiferromagnetic vector **L** and the axis C_3, and where φ is the angle between the direction of the projection of the antiferromagnetic vector **L** on the basal plane of the crystal and the vertical plane of symmetry.

On increase of the applied magnetic field, because of the term in the thermodynamic potential Φ with coefficient e, which is responsible for the transverse weak ferromagnetism $\sigma_D = e/B$ of the crystal, there occurs a rotation of the antiferromagnetic vector **L** and a change of the angle $\theta(H)$.[11,12] The occurrence of a component $\mathbf{L}_\perp$ of the antiferromagnetic vector in the basal plane of the crystal with increase of a magnetic field $\mathbf{H} \perp C_3$ is determined by the occurrence of a ferromagnetic moment of the specimen along the applied magnetic field;[8,9] the variation of the magnetic moment along the field, determined by the expression

$$m_y = \frac{e}{B}\sin\theta + \frac{H}{B}, \tag{4}$$

is linear with respect to the magnetic field, and the relation for the angle of rotation, determined by the expression

$$\sin\theta = \frac{H}{H_c^*}, \qquad H_c^* = \frac{aB - e^2}{e} L_0, \tag{5}$$

is also linear. The rotation of the antiferromagnetic vector **L** in the basal plane of the crystal is completed at magnetic field H_c^*.

When the value of $\sin\theta$ depends linearly on the applied magnetic field, the variation of the magnetic moment of the specimen along the axis C_3 is determined, as is evident from the expression (3), by the third power of the applied magnetic field. On substituting the expression (4) in (3), we find that the magnetic moment of the specimen along the axis C_3 is determined by the expression

$$m_z = \frac{d}{B} L_0 \cdot \left(\frac{H}{H_c^*}\right)^3 \cos 3\varphi. \tag{6}$$

The cubic dependence $M_z(H_\perp)$ determined by the expression (6) is confirmed by experiment (Fig. 5). The fact that the magnetic moment $M_\perp(H_\perp)$ of the specimen is practically independent of the orientation of H in the basal plane (Fig. 2) indicates a small value of the crystal anisotropy in this plane. It may then be assumed that the projection $\mathbf{L}_\perp$ of the antiferromagnetic vector on the basal plane of the crystal is perpendicular to the applied magnetic field. In this case, as is evident from the expression (3), the change of the value and sign of the magnetic moment along the axis C_3 on variation of the orientation of an applied magnetic field H in the basal plane of the crystal occurs with period 120°. On change of the orientation of the magnetic field H in the basal plane, the change of the value and sign of the magnetic moment along the axis C_3 occurs according to the law

$$M_z(\psi) = M_z(H_0)\cos 3\psi.$$

This law of variation of the magnetic moment along the axis C_3 with variation of the orientation of a magnetic field H in the basal plane is confirmed by the experiments presented in Figs. 3 and 4.

Thus it may be asserted that in antiferromagnetic $FeCl_2$ with a magnetic field oriented in the basal plane of the crystal, in addition to the magnetic moment $M_\perp(H_\perp)$ that occurs along the applied magnetic field, there occurs along the axis C_3 a magnetic moment $M_z(H_\perp)$ proportional to the third power of the applied magnetic field, and having periodicity 120° with variation of the orientation of $H_\perp$ in the basal plane. This magnetic moment originates as a result of the appearance of a component $L_\perp(H)$ of the antiferromagnetic vector **L** in the basal plane of the crystal. The orientation of the magnetic field H, of the magnetic moments $M_\perp(H_\perp)$ and $M_z(H_\perp)$, and of the components of the antiferromagnetic vector **L** are shown in Fig. 4 for various orientations of H in the basal plane of the crystal.

The occurrence, for certain orientations of the magnetic field in the basal plane of the crystal, of a component of the magnetic moment of the specimen along the axis C_3 is caused by nonequivalent rotation of the magnetic sublattices of $FeCl_2$ in a transverse magnetic field. Such nonequivalent rotation of the magnetic moments of the sublattices is determined by the action of an effective field resulting from the invariant of the fourth degree in γ and $\mathbf{m}$ in the thermodynamic potential that describes the magnetic properties of the crystal. Knowing the values of the magnetic susceptibilities for $FeCl_2$, we can determine the values of the effective field $H_E = (140 \pm 10)$ kOe, where $2H_e = BL_0$.

The authors thank P. L. Kapitza for his interest in the research, A. S. Borovik-Ramonov for direction of the research, and I. E. Dzyaloshinskiĭ, N. M. Kreĭnes, and V. A. Trunov for discussion of the results.

---

1) B. P. Konstantinov Leningrad Institute of Nuclear Physics, Academy of Sciences, USSR.

2) The authors are deeply grateful to G. A. Krutov for providing the single crystals.

---

[1] I. S. Jacobs and P. E. Lawrence, Phys. Rev. **164**, 866 (1967).

[2] P. Carrara, J. de Gunzbourg, and Y. Allain, J. Appl. Phys. **40**, 1035 (1969).

[3] M. C. Lanusse, P. Carrara, A. R. Fert, G. Mischler, and J. P. Redoulès, J. Phys. (Paris) **33**, 429 (1972).

[4] J. A. Nasser and F. Varret, AIP Conf. Proc. **24**, 59 (1965).

[5] V. A. Trunov, A. E. Egorov, R. P. Dmitriev, V. A. Ul'yanov, and M. E. Kravtsova, Pis'ma Zh. Eksp. Teor. Fiz. **20**, 312 (1974) [JETP Lett. **20**, 139 (1974)].

[6] A. N. Bazhan, A. S. Borovik-Romanov, and N. M. Kreĭnes, Prib. Tekh. Eksp. **16**, No. 1, 213 (1973) [Instrum. Exp. Tech. (USSR) **16**, No. 1, 261 (1973)].

[7] J. F. Dillon, Jr., E. Yi Chen, and H. J. Guggenheim, Solid State Commun. **16**, 371 (1975).

[8] A. N. Bazhan, Zh. Eksp. Teor. Fiz. **67**, 1520 (1974) [Sov. Phys. Phys. JETP **40**, 757 (1974)].

[9] I. E. Dzyaloshinskiĭ, Zh. Eksp. Teor. Fiz. **32**, 1547 (1957) [Sov. Phys. JETP **5**, 1259 (1957)].

[10] J. A. Nasser, J. Phys. (Paris) **40**, 51 (1979).

[11] N. M. Kreĭnes, Zh. Eksp. Teor. Fiz. **40**, 762 (1961) [Sov. Phys. JETP **13**, 534 (1961)].

[12] V. I. Ozhogin, Zh. Eksp. Teor. Fiz. **45**, 1687 (1963) [Sov. Phys. JETP **18**, 1156 (1964)].

Translated by W. F. Brown, Jr.

Kinetics of population and decay of highly excited states of TR^{3+} ions under conditions of strong incoherent interaction in the intermediate states

A. A. Glushko, V. V. Osiko, Yu. P. Timofeev, and I. A. Shcherbakov

P. N. Lebedev Physics Institute, USSR Academy of Sciences

(Submitted 17 December 1979)
Zh. Eksp. Teor. Fiz. **79**, 194–206 (July 1980)

The possible mechanisms of population of highly excited states of erbium ions by IR excitation into the absorption band of ytterbium ions is analyzed. The time dependences of the populations of these states following pulsed excitation are theoretically obtained for these mechanisms in a large temperature interval. The time evolutions of the populations of the highly excited states of erbium are measured in the dynamic range of variation of the radiation intensity, which reaches three orders of magnitude when they are excited into the ytterbium absorption band in polycrystalline $Y_{1-x-y}Yb_xEr_yOCl$ samples. All the intermediate levels that participate in the population of the highly excited states of erbium are selectively excited and their population and depletion kinetics are measured. The population mechanisms of these excited states are identified and switching from one mechanism to another in the course of time is observed. The theoretical and experimental results are in agreement. It is shown that a regime of strongly incoherent interaction in the low excited states of erbium and ytterbium is realized in the $Y_{0.87}Yb_{0.1}Er_{0.02}OCl$ system. The complicated time evolutions of the populations of the highly excited states of erbium are described by characteristic times that are determined by the regime of strong incoherent interaction of the erbium and ytterbium in low excited states.

PACS numbers: 31.50. + w

INTRODUCTION

The discovery of the interaction of trivalent ions of rare-earth elements (TR^{3+}) in excited states[1,2] is to a considerable degree the result of the use of kinetic methods to investigate the excitation-energy transformation in condensed media.[3] To distinguish between the mechanisms of interaction between the impurity system and the radiation, which brings about anti-Stokes radiation, many criteria were subsequently developed, based on an analysis of the optical spectra and of the dependences of the intensity on the impurity-particle concentration and on the excitation density.[1,2] It was reliably established as a result that in most cases the process of population of the highly excited states of TR^{3+} ions in condensed media is collective and proceeds via many stages. The branched structure of the states of the TR^{3+} ions, in conjunction with multistage character of the process, leads to an extraordinary variety of mechanisms whereby the highly excited states of these ions are populated. In many cases it remained unclear which of the TR^{3+} ion levels